

Graphical Nonlinear System Analysis

Thomas Chaffey¹, Fulvio Forni¹ and Rodolphe Sepulchre¹

Abstract—We use the recently introduced concept of a Scaled Relative Graph (SRG) to develop a graphical analysis of input-output properties of feedback systems. The SRG of a nonlinear operator generalizes the Nyquist diagram of an LTI system. In the spirit of classical control theory, important robustness indicators of nonlinear feedback systems are measured as distances between SRGs.

I. INTRODUCTION

The graphical analysis of a feedback system via the Nyquist diagram of its return ratio is a foundation of classical control theory. It underlies the analysis concept of stability margins and the design concept of loop shaping, which themselves provide the grounds for the gap metric [1], [2] and H_∞ control [3].

The Nyquist diagram also has a fundamental place in the theory of nonlinear systems of the Lur'e form (that is, systems composed of an LTI forward path in feedback with a static nonlinearity). The circle and Popov criteria allow the stability of a Lur'e system to be proved by verifying a geometric condition on the Nyquist diagram of the LTI component [4]. The geometric condition is determined by the properties of the static nonlinearity. Notably, only the Nyquist diagram of the LTI component is defined, owing to a lack of a suitable definition of phase for nonlinear systems. At best, the frequency response of a nonlinear system may be computed approximately. The describing function [5]–[7] gives rise to a family of Nyquist curves for a nonlinearity, parameterized by the amplitude of the input. Other efforts to generalize frequency response to nonlinear systems include the work of Pavlov, Wouw, and Nijmeijer [8] on Bode diagrams for convergent systems, and the recently introduced notions of nonlinear phase and singular angle by Chen *et al.* [9], [10].

In this paper, we show that the Scaled Relative Graph of Ryu, Hannah, and Yin [11] generalizes the Nyquist diagram of an LTI transfer function, and may be plotted for nonlinear input/output operators. The SRG has been introduced in the theory of optimization to visualize incremental properties of nonlinear operators, that is, properties that are measured between pairs of input/output trajectories, such as Lipschitz continuity and maximal monotonicity. Such properties may be verified by checking geometric conditions on the SRG of an operator. Algebraic manipulations to the operator correspond

to geometric manipulations to the SRG. The SRG gives rise to simple, intuitive and rigorous proofs of the convergence of many algorithms in convex optimization. Furthermore, the tool is particularly suited to proving tightness of convergence bounds, and has been used to prove novel tightness results [11], [12].

The objective of this paper is to provide a bridge between SRG analysis and the incremental input-output analysis of feedback systems [4]. Our main result (Theorem 2) establishes a generalization of the Nyquist theorem for stable nonlinear operators. Based on the homotopy argument central to IQC analysis [13], this result enables SRG analysis to address well-posedness issues – in contrast to [11] for example, where well-posedness of operators is *assumed*. In the context of nonlinear feedback system analysis, this result enables an elegant and classical definition of stability margins for nonlinear feedback systems. We illustrate the generality of the approach by recovering several classical results.

The second part of the paper aims at providing concrete illustrations of the theory. As a first step, we show that the SRG of an LTI system is derived from its Nyquist curve, and we also provide an analytical derivation of the SRG of scalar-valued static nonlinearities. Preliminary results were presented in the conference paper [14]. We then illustrate the application of SRG analysis to three representative examples from the literature. Our first example (Section VII) is a feedback loop involving delays and saturations, a classical benchmark of IQC system analysis [13]. Our SRG analysis provides an analytical bound on the feedback gain which guarantees stability, and closely matches previous numerical bounds obtained by IQC analysis. We stress however that the SRG analysis characterizes the incremental gain whereas previous bounds were non-incremental. We furthermore give an analytical bound on the incremental L_2 gain of the closed loop. This example illustrates the strength and potential of SRG analysis for verifying *incremental* properties, which is of considerable importance, even though it seems to have received little attention in IQC analysis [13], [15], [16]. Our second example illustrates SRG analysis in so-called cyclic feedback systems [17]–[20]. Here also SRG analysis suggests a strong potential: on top of providing an elegant graphical interpretation of existing results, we illustrate that SRG analysis provides analytical bounds on the incremental gain of the feedback system and stability margins against dynamical uncertainties. Our final example (Section IX) combines cascades and delays in the analysis of a congestion control model previously studied in [21]. Here again, SRG analysis provides novel bounds on the incremental gain, and generalizes the equilibrium-independent passivity analysis proposed in [21].

The research leading to these results has received funding from the European Research Council under the Advanced ERC Grant Agreement Switchlet n. 670645.

¹University of Cambridge, Department of Engineering, Trumpington Street, Cambridge CB2 1PZ, tlc37@cam.ac.uk, {f.forni, r.sepulchre}@eng.cam.ac.uk.

The rest of the paper is organised as follows. We begin by introducing some background material in Section II, before defining the SRG in Section III, and summarizing its main properties. Section IV presents our main theoretical results on the SRG analysis of feedback systems. Section V connects the SRG to the Nyquist diagram of an LTI transfer function, and Section VI describes the SRGs of important classes of static nonlinearities. Three detailed examples are then developed in Sections VII, VIII and IX. Some concluding remarks and areas for future research are given in Section X.

II. BACKGROUND AND PRELIMINARIES

A. Signal spaces, operators and relations

Let \mathcal{L} denote a Hilbert space, equipped with an inner product, $\langle \cdot | \cdot \rangle : \mathcal{L} \times \mathcal{L} \rightarrow \mathbb{C}$, and the induced norm $\|x\| := \sqrt{\langle x | x \rangle}$.

We will pay particular attention to Lebesgue spaces of square-integrable functions. Given a time axis, which for brevity we will always consider to be $\mathbb{R}_{\geq 0}$, and a field $\mathbb{F} \in \{\mathbb{R}, \mathbb{C}\}$, we define the space $L_2^n(\mathbb{F})$ by the set of signals $u : \mathbb{R}_{\geq 0} \rightarrow \mathbb{F}^n$ such that

$$\|u\| := \left(\int_0^\infty \bar{u}(t)u(t) dt \right)^{\frac{1}{2}} < \infty,$$

where $\bar{u}(t)$ denotes the conjugate transpose of $u(t)$. The inner product of $u, y \in L_2^n(\mathbb{F})$ is defined by

$$\langle u | y \rangle := \int_0^\infty \bar{u}(t)y(t) dt.$$

The Fourier transform of $u \in L_2^n(\mathbb{F})$ is defined as

$$\hat{u}(j\omega) := \int_0^\infty e^{-j\omega t} u(t) dt.$$

We omit the dimension and field when they are immaterial or clear from context.

For some $T \in \mathbb{R}_{\geq 0}$, define the truncation operator P_T by

$$(P_T u)(t) := \begin{cases} u(t) & t \leq T, \\ 0 & t > T, \end{cases}$$

where $t \in \mathbb{R}_{\geq 0}$ and u is an arbitrary signal. Define the *extension* of $L_2^n(\mathbb{F})$ [22], [23, p. 22], [4, p. 172] to be the space

$$L_{2,e}^n(\mathbb{F}) := \{u : \mathbb{R}_{\geq 0} \rightarrow \mathbb{F}^n \mid \|P_T u\| < \infty \text{ for all } T \in \mathbb{R}_{\geq 0}\}.$$

An *operator*, or *system*, on a space \mathcal{X} , is a possibly multi-valued map $R : \mathcal{X} \rightarrow \mathcal{X}$. The identity operator, which maps $u \in \mathcal{X}$ to itself, is denoted by I . The *graph*, or *relation*, of an operator, is the set $\{u, y \mid u \in \text{dom } R, y \in R(u)\} \subseteq \mathcal{X} \times \mathcal{X}$. We use the notions of an operator and its relation interchangeably, and denote them in the same way. The relation of an operator may be thought of as an input/output partition of a behavior [24, Def. 3.3.1].

The usual operations on functions can be extended to relations:

$$\begin{aligned} S^{-1} &= \{(y, u) \mid y \in S(u)\} \\ S + R &= \{(x, y + z) \mid (x, y) \in S, (x, z) \in R\} \\ SR &= \{(x, z) \mid \exists y \text{ s.t. } (x, y) \in R, (y, z) \in S\}. \end{aligned}$$

Note that S^{-1} always exists, but is not an inverse in the usual sense. In particular, it is in general not the case that $S^{-1}S = I$.

If, however, S is an invertible function, the relational inverse and functional inverse coincide, so the notation S^{-1} can be used without ambiguity.

An operator R on L_2 or $L_{2,e}$ is said to be *causal* if $P_T(R(u)) = P_T(R(P_T u))$ for all u .

B. Incremental input/output analysis

The input/output approach to nonlinear systems analysis originated in the dissertation of George Zames [25] and early work by Irwin Sandberg [26]. Noting that the amplification of a nonlinear system was, in general, dependent on the input, Zames introduced the notion of the *incremental gain* of a system, which characterizes the worst case amplification a system is capable of. Incremental properties feature heavily in Desoer and Vidyasagar's classic text [4]. The general pattern is that requiring a property to be verified for every possible input, rather than just a single distinguished input ($u = 0$, for example), leads to much stronger results, often comparable to the results that may be proved for linear systems. This is perhaps unsurprising, as any property of a linear system is automatically incremental. The study of properties relative to the zero input, however, have dominated nonlinear input/output theory since these early days.

We now define the input/output properties of systems considered in this paper. We begin with a definition of incremental stability.

Definition 1. Let $R : L_2 \rightarrow L_2$. The *incremental L_2 gain* of R is

$$\mu := \sup_{u_1, u_2 \in \text{dom } R} \frac{\|y_1 - y_2\|}{\|u_1 - u_2\|},$$

where $y_1 \in R(u_1)$, $y_2 \in R(u_2)$. If $\mu < \infty$, R is said to have *finite incremental L_2 gain*, or be *incrementally L_2 stable*. \lrcorner

The second class of properties relate to passivity.

Definition 2. Let $R : L_2 \rightarrow L_2$. Then:

- 1) R is said to be *incrementally positive* if

$$\langle u_1 - u_2 | y_1 - y_2 \rangle \geq 0$$

for all $u_1, u_2 \in \text{dom } R$ and $y_1 \in R(u_1), y_2 \in R(u_2)$.

- 2) R is said to be *λ -input-strict incrementally positive* if

$$\langle u_1 - u_2 | y_1 - y_2 \rangle \geq \lambda \|u_1 - u_2\|^2$$

for all $T \geq 0$, all $u_1, u_2 \in \text{dom } R$ and $y_1 \in R(u_1), y_2 \in R(u_2)$.

- 3) R is said to be *γ -output-strict incrementally positive* if

$$\langle u_1 - u_2 | y_1 - y_2 \rangle \geq \gamma \|y_1 - y_2\|^2$$

for all $u_1, u_2 \in \text{dom } R$ and $y_1 \in R(u_1), y_2 \in R(u_2)$. \lrcorner

For causal operators on L_2 , incremental positivity coincides with the stronger property of incremental passivity (the proof follows the same lines as [4, Lemma 2, p. 200]). In the language of optimization, incremental positivity is called *monotonicity*. Monotone operator theory originated in the study of networks of nonlinear resistors. The prototypical monotone operator was Duffin's *quasi-linear* resistor [27],

a resistor with increasing, but not necessarily linear, $i - v$ characteristic. The modern notion of a monotone operator was introduced by Minty [28], [29]. Following the influential paper of Rockafellar [30], monotone operators have become a cornerstone of optimization theory. Monotone operator methods have seen a surge of interest in the last decade, due to their applicability to large-scale and nonsmooth problems [31]–[34]. SRGs have been developed to prove convergence of these optimization methods.

Monotone operator theory is closely related to the classical input/output theory of nonlinear systems. All of the properties studied in the theory of monotone operators correspond to a property in input/output system theory, the difference being that the former are defined for an arbitrary Hilbert space, while the latter are defined on L_2 or $L_{2,e}$. Table I shows these equivalences.

III. SCALED RELATIVE GRAPHS

We define SRGs in the same way as Ryu, Hannah, and Yin [11], with the minor modification of allowing complex valued inner products.

Let \mathcal{L} be a Hilbert space. The angle between $u, y \in \mathcal{L}$ is defined as

$$\angle(u, y) := \arccos \frac{\operatorname{Re} \langle u | y \rangle}{\|u\| \|y\|} \in [0, \pi].$$

Let $R : \mathcal{L} \rightarrow \mathcal{L}$ be an operator. Given $u_1, u_2 \in \mathcal{U} \subseteq \mathcal{L}$, $u_1 \neq u_2$, define the set of complex numbers $z_R(u_1, u_2)$ by

$$z_R(u_1, u_2) := \left\{ \frac{\|y_1 - y_2\|}{\|u_1 - u_2\|} e^{\pm j \angle(u_1 - u_2, y_1 - y_2)} \mid y_1 \in R(u_1), y_2 \in R(u_2) \right\}.$$

If $u_1 = u_2$ and there are corresponding outputs $y_1 \neq y_2$, then $z_R(u_1, u_2)$ is defined to be $\{\infty\}$. If R is single valued at u_1 , $z_R(u_1, u_1)$ is the empty set.

The *Scaled Relative Graph* (SRG) of R over $\mathcal{U} \subseteq \mathcal{L}$ is then given by

$$\operatorname{SRG}_{\mathcal{U}}(R) := \bigcup_{u_1, u_2 \in \mathcal{U}} z_R(u_1, u_2).$$

If $\mathcal{U} = \mathcal{L}$, we write $\operatorname{SRG}(R) := \operatorname{SRG}_{\mathcal{L}}(R)$.

If R is linear and $\operatorname{dom} R$ is a linear subspace of \mathcal{L} , $Ru_1 - Ru_2 = R(u_1 - u_2) = Rv$ for some $v \in \operatorname{dom} R$, and we can define

$$z_R(v) := \frac{\|Rv\|}{\|v\|} e^{\pm j \angle(v, Rv)}$$

and

$$\operatorname{SRG}_{\operatorname{dom} R}(R) := \{z_R(v) \mid v \in \operatorname{dom} R, v \neq 0\}.$$

In the special case that R is linear and time invariant with transfer function $R(s)$, and $v(t) = e^{j\omega t}$, $\lim_{T \rightarrow \infty} \|R(P_T v)\| / \|P_T v\| = |R(j\omega)|$ and $\lim_{T \rightarrow \infty} \angle(P_T v, R(P_T v)) = |\arg R(j\omega)|$ (where $\arg R(j\omega)$ is measured between $-\pi$ and π). Thus the gain and phase of the SRG generalize the classical notions of the gain and phase of an LTI transfer function.

A. System properties from SRGs

If \mathcal{A} is a class of operators, we define the SRG of \mathcal{A} by

$$\operatorname{SRG}(\mathcal{A}) := \bigcup_{R \in \mathcal{A}} \operatorname{SRG}(R).$$

Note that a class of operators can be a single operator.

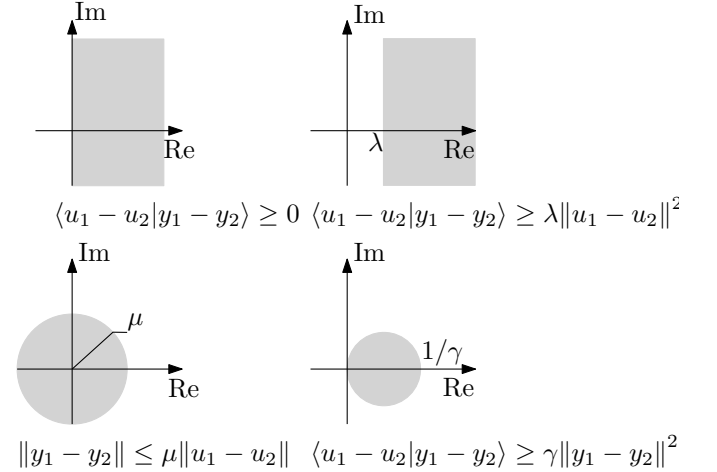
A class \mathcal{A} , or its SRG, is called *SRG-full* if

$$R \in \mathcal{A} \iff \operatorname{SRG}(R) \subseteq \operatorname{SRG}(\mathcal{A}).$$

By construction, the implication $R \in \mathcal{A} \implies \operatorname{SRG}(R) \subseteq \operatorname{SRG}(\mathcal{A})$ is true. The value of SRG-fullness is in the reverse implication: $\operatorname{SRG}(R) \subseteq \operatorname{SRG}(\mathcal{A}) \implies R \in \mathcal{A}$. This allows class membership to be tested graphically. If \mathcal{A} is the class of systems with a particular system property, SRG-fullness of \mathcal{A} allows this property to be verified for a particular operator R by plotting its SRG. If $\operatorname{SRG}(R) \subseteq \operatorname{SRG}(\mathcal{A})$, R has the property.

The following proposition gives the SRGs of the classical system properties introduced in Section II-B.

Proposition 1. *The SRGs of incrementally positive systems (top left), input-strict incrementally positive systems (top right), output-strict incrementally positive systems (bottom right) and incrementally L_2 bounded systems (bottom left) are shown below.*



All of these classes are SRG-full.

Proof. These SRGs are proved in [11], and all of the shapes follow from quick calculations. SRG-fullness follows from [11, Thm. 3.5]. \square

SRG-fullness of the classes of Proposition 1 means, for example, that if the SRG of a system lies in the right half plane, the system is incrementally positive, and if the SRG of a system is bounded, the system has finite incremental L_2 gain. These are reminiscent of the facts that an LTI system is passive if its Nyquist diagram lies in the right half plane, and has finite H_∞ norm if its Nyquist diagram is bounded. We will show in Section V that Proposition 1 is indeed a generalization of these classical facts.

The properties of finite incremental L_2 gain and incremental positivity are particular examples of incremental Integral Quadratic Constraints (IQCs) [13]. A striking corollary of Ryu,

property	L_2	$L_{2,e}$	Hilbert
$\ y_1 - y_2\ \leq \mu \ u_1 - u_2\ $	finite incremental gain	finite incremental gain*	Lipschitz
$\langle u_1 - u_2 y_1 - y_2 \rangle \geq 0$	incremental positivity	incremental passivity*	monotonicity
$\langle u_1 - u_2 y_1 - y_2 \rangle \geq \lambda \ u_1 - u_2\ ^2$	incremental input-strict positivity	incremental input-strict passivity*	strong monotonicity or coercivity
$\langle u_1 - u_2 y_1 - y_2 \rangle \geq \gamma \ y_1 - y_2\ ^2$	incremental output-strict positivity	incremental output-strict passivity*	cocoercivity

TABLE I: A partial bilingual dictionary from input/output system theory to monotone operator theory. The first column gives properties between pairs of inputs u_1, u_2 and the corresponding outputs y_1, y_2 . Greek letters denote positive scalars. The second and third columns give the system theory names of properties of operators on either L_2 or $L_{2,e}$, as defined by [4]. The names in the second column (*) apply if the property holds for every truncation $\langle P_T u_1 - P_T u_2 | P_T y_1 - P_T y_2 \rangle$, $T > 0$. The fourth column gives the names of these properties in monotone operator theory, for operators on an arbitrary Hilbert space - see, for example, [11].

Hannah, and Yin [11, Thm. 3.5] is that any SRG defined by a static incremental IQC is SRG-full.

Proposition 2. *Let $u_i(t)$ denote the input to an arbitrary operator on L_2 , and $y_i(t)$ denote a corresponding output. Let $\Delta u = u_1 - u_2$ and $\Delta y = y_1 - y_2$, and $\hat{x}(\omega)$ denote the Fourier transform of signal $x(t)$. Then the classes of operators which obey either of the constraints*

$$\int_{-\infty}^{\infty} \begin{pmatrix} \Delta \hat{u}(\omega) \\ \Delta \hat{y}(\omega) \end{pmatrix}^\top \begin{pmatrix} a & b \\ c & d \end{pmatrix} \begin{pmatrix} \Delta \hat{u}(\omega) \\ \Delta \hat{y}(\omega) \end{pmatrix} d\omega \geq 0, \quad (1)$$

$$\int_0^{\infty} \begin{pmatrix} \Delta u(t) \\ \Delta y(t) \end{pmatrix}^\top \begin{pmatrix} a & b \\ c & d \end{pmatrix} \begin{pmatrix} \Delta u(t) \\ \Delta y(t) \end{pmatrix} dt \geq 0, \quad (2)$$

where $a, b, c, d \in \mathbb{R}$, are SRG-full.

Proof. Equation (1) gives

$$a \|\Delta \hat{u}\|^2 + (b+c) \langle \Delta \hat{u} | \Delta \hat{y} \rangle + d \|\Delta \hat{y}\|^2 \geq 0.$$

By Parseval's theorem, this is equivalent to

$$a \|\Delta u\|^2 + (b+c) \langle \Delta u | \Delta y \rangle + d \|\Delta y\|^2 \geq 0,$$

which is also implied by (2). The result then follows from [11, Thm. 3.5]. \square

A class of operators defined by a geometric region is SRG-full.

Proposition 3. *Let $\mathcal{C} \subseteq \mathbb{C}$. The class of operators \mathcal{A} defined by*

$$\mathcal{A} := \{R \text{ an operator} \mid \text{SRG}(R) \subseteq \mathcal{C}\}$$

is SRG-full.

Proof. The definition of \mathcal{A} can be written as

$$R \in \mathcal{A} \iff \text{SRG}(R) \subseteq \mathcal{C},$$

which is the definition of SRG-fullness. \square

This fact is particularly useful for system analysis, as it allows the SRG of an operator to be over-approximated by a geometric region if, for example, the precise SRG is unknown, or the SRG does not obey the properties necessary to apply

a theorem. Over-approximating an SRG simply amounts to making the analysis more conservative.

B. Interconnections

Under mild conditions on the SRG, system interconnections correspond to geometric manipulations of their SRGs. These interconnection results are proved by Ryu, Hannah, and Yin [11] in Theorems 4.1-4.5. We recall the statements of these theorems in the following five propositions.

Proposition 4. *If \mathcal{A} and \mathcal{B} are SRG-full, then $\mathcal{A} \cap \mathcal{B}$ is SRG-full, and*

$$\text{SRG}(\mathcal{A} \cap \mathcal{B}) = \text{SRG}(\mathcal{A}) \cap \text{SRG}(\mathcal{B}).$$

Proposition 5. *Let $\alpha \in \mathbb{R}, \alpha \neq 0$. If \mathcal{A} is a class of operators,*

$$\text{SRG}(\alpha \mathcal{A}) = \text{SRG}(\mathcal{A} \alpha) = \alpha \text{SRG}(\mathcal{A}),$$

$$\text{SRG}(I + \mathcal{A}) = 1 + \text{SRG}(\mathcal{A}).$$

Furthermore, if \mathcal{A} is SRG-full, then $\alpha \mathcal{A}$, $\mathcal{A} \alpha$ and $I + \mathcal{A}$ are SRG-full.

We define inversion in the complex plane by the Möbius transformation $re^{j\omega} \mapsto (1/r)e^{j\omega}$. This is “inversion in the unit circle”: points outside the unit circle map to the inside, and vice versa. The points 0 and ∞ are exchanged under inversion.

Proposition 6. *If \mathcal{A} is a class of operators, then*

$$\text{SRG}(\mathcal{A}^{-1}) = (\text{SRG}(\mathcal{A}))^{-1}.$$

Furthermore, if \mathcal{A} is SRG-full, then \mathcal{A}^{-1} is SRG-full.

Define the line segment between $z_1, z_2 \in \mathbb{C}$ as $[z_1, z_2] := \{\alpha z_1 + (1-\alpha)z_2 \mid \alpha \in [0, 1]\}$. A class of operators \mathcal{A} is said to satisfy the *chord property* if $z \in \text{SRG}(\mathcal{A}) \setminus \{\infty\}$ implies $[z, \bar{z}] \subseteq \text{SRG}(\mathcal{A})$.

Proposition 7. *Let \mathcal{A} and \mathcal{B} be classes of operators, such that $\infty \notin \text{SRG}(\mathcal{A})$ and $\infty \notin \text{SRG}(\mathcal{B})$. Then:*

- 1) *if \mathcal{A} and \mathcal{B} are SRG-full, then $\text{SRG}(\mathcal{A} + \mathcal{B}) \supseteq \text{SRG}(\mathcal{A}) + \text{SRG}(\mathcal{B})$.*
- 2) *if either \mathcal{A} or \mathcal{B} satisfies the chord property, then $\text{SRG}(\mathcal{A} + \mathcal{B}) \subseteq \text{SRG}(\mathcal{A}) + \text{SRG}(\mathcal{B})$.*

Under additional assumptions, ∞ can be allowed - see the discussion following [11, Thm. 4.4].

Define the *right-hand arc*, $\text{Arc}^+(z, \bar{z})$, between z and \bar{z} to be the arc between z and \bar{z} with centre on the origin and real part greater than or equal to $\text{Re}(z)$. The *left-hand arc*, $\text{Arc}^-(z, \bar{z})$, is defined the same way, but with real part less than or equal to $\text{Re}(z)$. Formally,

$$\begin{aligned} \text{Arc}^+(z, \bar{z}) &:= \{re^{j(1-2\vartheta)\phi} \mid z = re^{j\phi}, \\ &\quad \phi \in (-\pi, \pi], \vartheta \in [0, 1], r \geq 0\}, \\ \text{Arc}^-(z, \bar{z}) &:= -\text{Arc}^+(-z, -\bar{z}). \end{aligned}$$

A class of operators \mathcal{A} is said to satisfy the *right hand (resp. left hand) arc property* if, for all $z \in \text{SRG}(\mathcal{A})$, $\text{Arc}^+(z, \bar{z}) \in \text{SRG}(\mathcal{A})$ (resp. $\text{Arc}^-(z, \bar{z}) \in \text{SRG}(\mathcal{A})$).

Proposition 8. *Let \mathcal{A} and \mathcal{B} be classes of operators, such that $\infty \notin \text{SRG}(\mathcal{A})$, $\mathcal{A} \neq \emptyset$, $\infty \notin \text{SRG}(\mathcal{B})$ and $\mathcal{B} \neq \emptyset$. Then:*

- 1) *if \mathcal{A} and \mathcal{B} are SRG-full, then $\text{SRG}(\mathcal{A}\mathcal{B}) \supseteq \text{SRG}(\mathcal{A})\text{SRG}(\mathcal{B})$.*
- 2) *if either \mathcal{A} or \mathcal{B} satisfies an arc property, then $\text{SRG}(\mathcal{A}\mathcal{B}) \subseteq \text{SRG}(\mathcal{A})\text{SRG}(\mathcal{B})$.*

Under additional assumptions, ∞ and \emptyset can be allowed - see the discussion following [11, Thm. 4.5].

C. Scaled graphs about particular solutions

Scaled relative graphs capture the behavior of an operator with respect to any possible operating point. However, the behavior about one or several specific inputs (for example, stable equilibria) may be of particular interest. The methods of this paper apply equally to the analysis of properties with respect to particular inputs, via the *scaled graph* (SG). For notational convenience, we only define the SG over the full space, but the SG can be restricted to a subset of the input space in the same way as the SRG.

Definition 3. Let $R : \mathcal{L} \rightarrow \mathcal{L}$. The *scaled graph* of R over \mathcal{L} with respect to the input u^* is

$$\text{SG}_{u^*}(R) := \bigcup_{u \in \mathcal{L}} z_R(u, u^*).$$

┘

Note that the SG of an LTI operator with respect to any input is equal to its SRG.

The graphical algebra of SRGs applies to SGs with very little modification - the only requirement is that interconnected SGs are defined with respect to compatible inputs. In the remainder of this section, we highlight the difference between incremental and input-specific properties, using the example of positivity.

Definition 4. An operator $H : L_2 \rightarrow L_2$ is said to be *positive about $u^* \in L_2$* if, for all $u \in L_2$, $y \in H(u)$ and $y^* \in H(u^*)$, $\langle u - u^* | y - y^* \rangle > 0$.

┘

From this definition, it follows immediately that an operator is positive about u^* if and only if its SG about u^* belongs to the closed right half plane. However, this does not mean

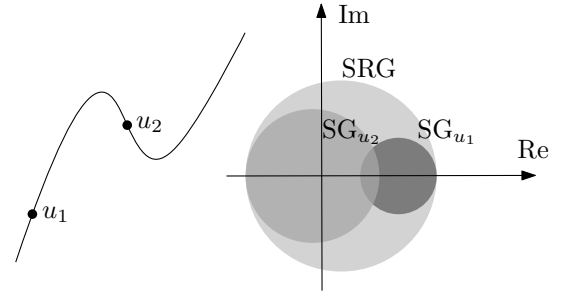


Fig. 1: On the left is the $i-v$ characteristic of a resistor with a region of negative resistance. The resistor is positive about some operating points (including u_1), but not about others (such as u_2). On the right are the SGs computed at u_1 and u_2 , as well as the SRG.

its SG about any other input necessarily lies in the right half plane - Figure 1 gives such an example.

Taking the union of SGs over multiple trajectories allows properties that lie between trajectory-dependent and incremental to be verified. For example, Hines, Arcak, and Packard [35] define *equilibrium-independent passivity* to be passivity with respect to every constant input to the system (under assumptions on the system that ensure that there is a constant output for every constant input). This can be verified by checking that the union of SGs over constant inputs lies in the right half plane.

IV. FEEDBACK ANALYSIS WITH SCALED RELATIVE GRAPHS

In this section, we demonstrate the use of scaled relative graphs for the stability analysis of feedback interconnections. We begin by using the SRG to generalize the Nyquist criterion to a stable nonlinear operator in unity gain negative feedback, and introduce a nonlinear stability margin. We then formulate a general stability theorem by inflating the point -1 to the negative of the SRG of an operator in the feedback path, and show that this theorem encompasses both the incremental small gain and incremental passivity theorems.

This stability theorem relies on viewing a feedback interconnection as the inverse of a parallel interconnection. The conditions of the theorem ensure that the parallel interconnection has a strictly positive lower bound on its incremental gain; it then follows that its inverse has an upper bound on its incremental gain. In order to show that a feedback interconnection leads to a well-defined operator, we use a homotopy argument similar to Megretski and Rantzer [13]. We place a gain $\tau \in [0, 1]$ in the feedback loop, and assume stability for $\tau = 0$ (no feedback). We then use SRGs to show stability for every $\tau \in (0, 1]$, which implies that there is no loss of stability as the feedback is introduced. This allows us to use SRG analysis to prove not only stability, but also well-posedness.

A. A Nyquist stability criterion for stable nonlinear operators

The Nyquist criterion characterizes the stability of a transfer function L in unity gain negative feedback (Figure 2) in terms

of the distance between the Nyquist diagram of L and the point -1 . This distance is called the *stability margin*, and is the inverse of the H_∞ norm of the sensitivity transfer function [36, p. 50]. In this section, we show that the Nyquist criterion and stability margin can be generalized to stable nonlinear operators by replacing the Nyquist diagram with an SRG. For such stable nonlinear operators, the closed loop system is stable if the SRG of the loop operator leaves -1 on the left.

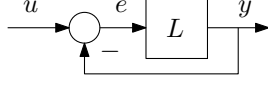


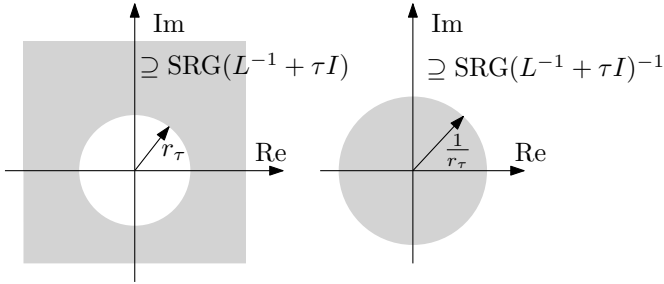
Fig. 2: Unity gain negative feedback around the relation L .

Theorem 1. Let $L : L_2 \rightarrow L_2$ be an operator with finite incremental L_2 gain. The closed loop operator shown in Figure 2 maps L_2 to L_2 and has finite incremental L_2 gain from u to y if

$$0 \notin 1 + \tau \text{SRG}(L) \quad \text{for all } \tau \in (0, 1]. \quad (3)$$

The closed loop gain from u to e in Figure 2 is bounded above by $1/s_m$, where s_m is the shortest distance between $\text{SRG}(L)$ and -1 .

Proof. We place a gain of τ in the feedback path, and show that the mapping from τ to the incremental gain from u to y is continuous if (3) holds. The operator from u to y is given by $(L^{-1} + \tau I)^{-1}$. Let the distance between $\text{SRG}(L^{-1})$ and $-\tau$ be $r_\tau > 0$. Then $\text{SRG}(L^{-1} + \tau I)$ is at least a distance of r_τ from the origin, so its inverse is at most $1/r_\tau$ from the origin, giving a bound of $1/r_\tau$ on the incremental gain from u to y , as illustrated below. Condition (3) guarantees that $r_\tau > 0$ for all $\tau \in (0, 1]$.



Let $\varepsilon > 0$ be smaller than r_τ . Then there exists a δ (positive or negative) such that, if τ is changed to $\tau + \delta$, the distance r_τ decreases by ε . Furthermore, as $\varepsilon \rightarrow 0$, $\delta \rightarrow 0$. This is a statement of the fact that the distance between a set and a point varies continuously with the position of the point. The closed loop incremental gain bound then increases to $1/(r_\tau - \varepsilon)$. This is bounded provided $\varepsilon < r_\tau$ (in which case δ small enough that $-(\tau + \delta)$ doesn't intersect $\text{SRG}(L^{-1})$) and approaches r_τ as $\delta \rightarrow 0$. This shows continuity from τ to the closed loop incremental gain from u to y , and shows that finite incremental gain is preserved provided $\text{SRG}(L^{-1})$ never intersects $-1/\tau$. In particular, all inputs in L_2 continue to map to outputs in L_2 . We conclude finite incremental gain from u to y by setting $\tau = 1$.

To prove the second part of the theorem, note that the relation from u to e is given by

$$e = (I + L)^{-1}u.$$

If $\text{SRG}(I + L)$ is bounded away from 0 by a distance s_m , then $(I + L)^{-1}$ has an L_2 gain bound of $1/s_m$. \square

B. A general feedback stability theorem

The Nyquist stability criterion presented in the previous section can be generalized to allow a second nonlinear operator in the feedback path, by inflating the point -1 into the SRG of the feedback operator. The following theorem encompasses the classical small gain and passivity theorems as special cases.

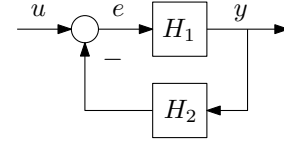


Fig. 3: Negative feedback interconnection of H_1 and H_2 .

Let \mathcal{H} be a class of operators. By $\bar{\mathcal{H}}$, we will denote a class of operators such that $\mathcal{H} \subseteq \bar{\mathcal{H}}$ and $\text{SRG}(\bar{\mathcal{H}})$ satisfies the chord property.

Theorem 2. Consider the feedback interconnection shown in Figure 3 between any pair of operators $H_1 \in \mathcal{H}_1$ and $H_2 \in \mathcal{H}_2$, where \mathcal{H}_1 is a class of operators on L_2 with finite incremental gain, and \mathcal{H}_2 is a class of operators on L_2 . If, for all $\tau \in (0, 1]$,

$$\text{SRG}(\mathcal{H}_1)^{-1} \cap -\tau \text{SRG}(\bar{\mathcal{H}}_2) = \emptyset,$$

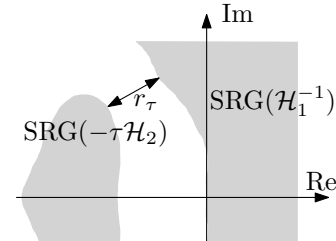
then the feedback interconnection maps L_2 to L_2 and has an incremental L_2 gain bound from u to y of $1/r_m$, where r_m is the shortest distance between $\text{SRG}(\mathcal{H}_1^{-1})$ and $-\text{SRG}(\bar{\mathcal{H}}_2)$.

The choice of which SRG to over-approximate is arbitrary. In the theorem, we have chosen $\text{SRG}(\bar{\mathcal{H}}_2)$, but it could just as well be $\text{SRG}(\mathcal{H}_1^{-1})$.

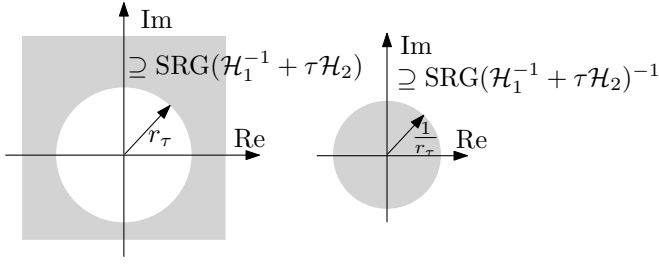
Proof of Theorem 2. For a gain of τ in the feedback path, the class of operators from u to y is given by

$$(\mathcal{H}_1^{-1} + \tau \mathcal{H}_2)^{-1}.$$

Suppose there exists a positive number r_τ such that $|z - w| \geq r_\tau$ for all $z \in \text{SRG}(\mathcal{H}_1^{-1})$, $w \in \text{SRG}(-\tau \bar{\mathcal{H}}_2)$.



Since $\text{SRG}(\mathcal{H}_1^{-1} + \tau \mathcal{H}_2) \subseteq \text{SRG}(\mathcal{H}_1^{-1}) + \tau \text{SRG}(\bar{\mathcal{H}}_2)$, where $H_2 \in \bar{\mathcal{H}}_2$, it follows that $\text{SRG}(\mathcal{H}_1^{-1} + \tau \mathcal{H}_2)$ is bounded away from zero by a distance of r_τ for all $H_2 \in \bar{\mathcal{H}}_2$. In particular, this holds for every operator $H_2 \in \mathcal{H}_2$.



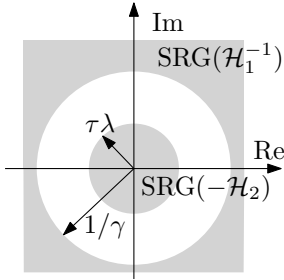
Applying the inverse transformation gives an incremental L_2 gain bound of $1/r_\tau$.

Ensuring this holds for all $\tau \in (0, 1]$ means the finite incremental gain of \mathcal{H}_1 is never lost, so the feedback interconnection remains defined on L_2 . r_m corresponds to r_1 . \square

One case where the criteria of Theorem 2 are automatically satisfied is the classical small gain setting.

Corollary 1. *Consider the feedback interconnection shown in Figure 3 between any pair of operators $H_1 \in \mathcal{H}_1$ and $H_2 \in \mathcal{H}_2$, where \mathcal{H}_1 and \mathcal{H}_2 are the classes of operators on L_2 with finite incremental L_2 gain bounds of γ and λ , respectively. If $\gamma\lambda < 1$, then the feedback interconnection maps L_2 to L_2 and has an incremental L_2 gain bound from u to y of $\gamma/(1-\gamma\lambda)$.*

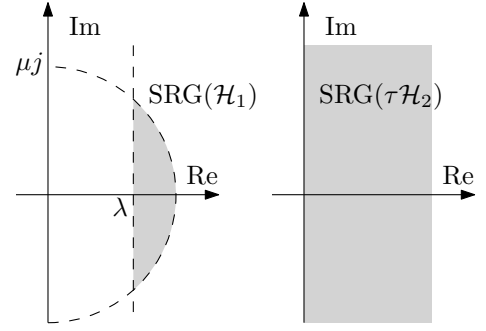
Proof. The result follows directly from Theorem 2. The conditions of the theorem are shown to be satisfied by the geometry below.



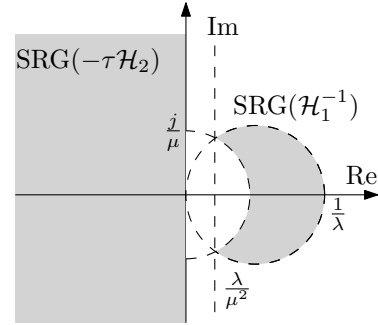
The second case where the conditions of Theorem 2 are automatically satisfied is in the feedback interconnection of incrementally positive systems. The classical incremental passivity theorem [22] is proved in the following corollary.

Corollary 2. *Consider the feedback interconnection shown in Figure 3 between any pair of operators $H_1 \in \mathcal{H}_1$ and $H_2 \in \mathcal{H}_2$, where \mathcal{H}_1 is the class of operators which are γ -output-strict incrementally positive operators which have an incremental L_2 gain bound of μ , and \mathcal{H}_2 is the class of incrementally positive operators. Assume $\lambda > 0$. Then the feedback interconnection maps L_2 to L_2 and has an incremental L_2 gain bound from u to y of μ^2/λ .*

Proof. The SRGs of H_1 and H_2 are contained in the SRGs shown below. Note that these both satisfy the chord property.



The SRG of the inverse of the class of λ -input-strict incrementally positive operators is the circle with centre $1/(2\lambda)$ and radius $1/(2\lambda)$ (Proposition 1). This circle is parameterized as $\{(1/\lambda)\cos(\vartheta)\exp(j\vartheta), | 0 \leq \vartheta \leq 2\pi\}$. The semicircle with centre at the origin, positive real part and radius μ , which is the SRG of the class of incrementally positive operators with an incremental L_2 gain bound of μ , is parameterized as $\{\mu\exp(j\phi), | -\pi/2 \leq \phi \leq \pi/2\}$. The result then follows from Theorem 2 and the geometry below.



\square

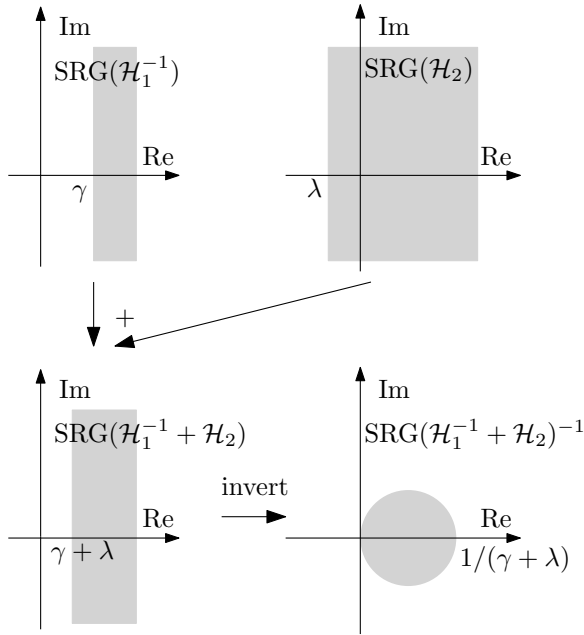
Corollary 2 characterizes the incremental gain of the closed loop. We can also characterize the incremental positivity of the closed loop, with another form of the classical passivity theorem. The following theorem generalizes [14, Prop. 8].

Theorem 3. *Consider the feedback interconnection shown in Figure 3 between any pair of operators $H_1 \in \mathcal{H}_1$ and $H_2 \in \mathcal{H}_2$, where \mathcal{H}_1 is the class of operators which are γ -output-strict incrementally positive, and \mathcal{H}_2 is the class of operators which are λ -input-strict incrementally positive. If*

$$\lambda + \gamma \geq 0,$$

then the operator from u to y is $(\gamma + \lambda)$ -output-strict incrementally positive.

Proof. Assume, without loss of generality, that $\lambda < 0$. We first prove the case where $\lambda + \gamma > 0$. This follows from the geometry shown below.



The case where $\lambda + \gamma = 0$ then follows by taking the limit $\lambda \rightarrow -\gamma$, and allowing the radius of the circle in the final panel above to tend to ∞ . \square

The definition of a stability margin for nonlinear operators leads us naturally to pose an “ H_∞ design problem”, in the same vein as Zames [3], to do with the maximization of the stability margin over a set of admissible controllers. A generalization of the H_∞ design question to nonlinear operators is as follows: given a plant G (modelled by an operator on L_2) in feedback with an uncertain block Δ known to be bounded by a particular SRG, design a controller C to maximize the distance between $\text{SRG}(CG)^{-1}$ and $-\text{SRG}(\Delta)$.

V. THE SCALED RELATIVE GRAPH OF AN LTI TRANSFER FUNCTION

In this section, we show that the SRG of a stable LTI transfer function is the convex hull of its Nyquist diagram, under the Beltrami-Klein mapping. We first presented this result in [14], and it was noted by Pates [37] that this is a special case of a more general phenomenon involving the numerical range of a linear operator. This allows computational methods for the numerical range to be applied directly to computation of the boundary of an SRG.

We begin by introducing some preliminaries from hyperbolic geometry in Section V-A, before giving the main result in Section V-B.

A. Hyperbolic geometry

We recall some necessary details from hyperbolic geometry. The notation is consistent with Huang, Ryu, and Yin [38].

Definition 5. Let $z_1, z_2 \in \mathbb{C}_{\text{Im} \geq 0} := \{z \in \mathbb{C} \mid \text{Im}(z) \geq 0\}$, the upper half complex plane. We define the following sets:

- 1) $\text{Circ}(z_1, z_2)$ is the circle through z_1 and z_2 with centre on the real axis. If $\text{Re}(z_1) = \text{Re}(z_2)$, this is defined as the infinite line passing through z_1 and z_2 .

- 2) $\text{Arc}_{\min}(z_1, z_2)$ is the arc of $\text{Circ}(z_1, z_2)$ in $\mathbb{C}_{\text{Im} \geq 0}$. If $\text{Re}(z_1) = \text{Re}(z_2)$, then $\text{Arc}_{\min}(z_1, z_2)$ is $[z_1, z_2]$.
- 3) Given $z_1, \dots, z_m \in \mathbb{C}_{\text{Im} \geq 0}$, the *arc-edge polygon* is defined by: $\text{Poly}(z_1) := \{z_1\}$ and $\text{Poly}(z_1, \dots, z_m)$ is the smallest simply connected set containing S , where

$$S = \bigcup_{i,j=1 \dots m} \text{Arc}_{\min}(z_i, z_j). \quad \lrcorner$$

Note that, as $\text{Poly}(z_1, \dots, z_{m-1}) \subseteq \text{Poly}(z_1, \dots, z_{m-1}, z_m) \subseteq \mathbb{C}_{\text{Im} \geq 0}$, the set $\text{Poly}(Z)$, where Z is a countably infinite sequence of points in $\mathbb{C}_{\text{Im} \geq 0}$, is well defined as the limit $\lim_{m \rightarrow \infty} \text{Poly}(Z_m)$, where Z_m is the length m truncation of Z (see [39, p. 111]).

Definition 5 forms the basis of the Poincaré half plane model of hyperbolic geometry. Under the Beltrami-Klein mapping, $f \circ g$, where

$$f(z) = \frac{2z}{1 + |z|^2},$$

$$g(z) = \frac{z - j}{z + j},$$

$\mathbb{C}_{\text{Im} \geq 0}$ is mapped onto the unit disc, and $\text{Arc}_{\min}(z_1, z_2)$ is mapped to a straight line segment. We make the following definitions of convexity and the convex hull in the Poincaré half plane model.

Definition 6. A set $S \subseteq \mathbb{C}_{\text{Im} \geq 0}$ is called *hyperbolic-convex* or *h-convex* if

$$z_1, z_2 \in S \implies \text{Arc}_{\min}(z_1, z_2) \in S.$$

Given a set of points $P \in \mathbb{C}_{\text{Im} \geq 0}$, the *h-convex hull* of P is the smallest h-convex set containing P . \lrcorner

Note that h-convexity is equivalent to Euclidean convexity under the Beltrami-Klein mapping. $\text{Arc}_{\min}(z_1, z_2)$ is the minimal geodesic between z_1 and z_2 under the Poincaré metric, so h-convexity may be thought of as geodesic convexity with respect to this metric. We recall the following useful lemma of Huang, Ryu, and Yin [38].

Lemma 1. (Lemma 2.1 [38]): Given a sequence of points $Z \in \mathbb{C}_{\text{Im} \geq 0}$, $\text{Poly}(Z)$ is h-convex.

In our terminology, given a sequence of points $Z \in \mathbb{C}_{\text{Im} \geq 0}$, $\text{Poly}(Z)$ is the h-convex hull of Z .

B. SRGs of LTI transfer functions

Let $g: L_2 \rightarrow L_2$ be linear and time invariant, and denote its transfer function by $G(s)$. g maps a complex sinusoid $u(t) = ae^{j\omega t}$ to the complex sinusoid $y(t) = a|G(j\omega)|e^{j\angle G(j\omega) + j\omega t}$. These signals do not belong to L_2 , but are treated as limits of sequences in L_2 . Precisely, we define the points on the SRG corresponding to sinusoidal signals by taking the gain and phase to be

$$\lim_{T \rightarrow \infty} \frac{\|P_T y\|}{\|P_T u\|}$$

$$\lim_{T \rightarrow \infty} \angle(P_T u, P_T y).$$

Both these limits exist when u and y are sinusoidal. The Nyquist diagram $\text{Nyquist}(G)$ of an operator $g : L_2(\mathbb{C}) \rightarrow L_2(\mathbb{C})$ is the locus of points $\{G(j\omega) | \omega \in \mathbb{R}\}$.

Theorem 4. *Let $g : L_2(\mathbb{C}) \rightarrow L_2(\mathbb{C})$ be linear and time invariant, with transfer function $G(s)$. Then $\text{SRG}(g) \cap \mathbb{C}_{\text{Im} \geq 0}$ is the h -convex hull of $\text{Nyquist}(G) \cap \mathbb{C}_{\text{Im} \geq 0}$.*

The proof of Theorem 4 is closely related to the proof of Huang, Ryu, and Yin [38, Thm. 3.1], and may be found in Appendix I. A consequence of Theorem 4 is that the SRG of an LTI operator is bounded by its Nyquist diagram. For example, the SRG of the transfer function $1/(s^3 + 5s^2 + 2s + 1)$ is illustrated in 4. Further examples are given in [14].

Given Theorem 4, we recover two familiar properties of the Nyquist diagram as special cases of Proposition 1, namely that passivity is equivalent to the Nyquist diagram lying in the right half plane, and the H_∞ gain is the maximum magnitude of the Nyquist diagram.

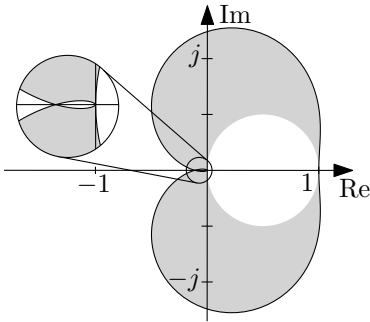


Fig. 4: SRG of the transfer function $1/(s^3 + 5s^2 + 2s + 1)$. The black curve is its Nyquist diagram, the grey region is the SRG.

VI. SCALED RELATIVE GRAPHS OF STATIC NONLINEARITIES

LTI systems map complex sinusoids to complex sinusoids, and the behavior of an LTI system on L_2 can be fully characterized by its behavior on complex sinusoids.

Similarly, static nonlinearities map square waves to square waves. Here, we show that the behavior of single input, single output static nonlinearities on L_2 , insofar as it is captured by the scaled relative graph, is fully characterized by their behavior on a two-dimensional subspace of L_2 spanned by two Haar wavelets (truncations of a square wave to a single period). In particular, we show that the SRGs of the saturation and ReLU are identical, and closely related to the SRG of a first order lag. The use of square waves allows us to test the effect of different input amplitudes on the output, which is analogous to the use of sinusoids to test the effect of different input frequencies on the output of an LTI system.

Proposition 9. *Suppose $S : L_2 \rightarrow L_2$ is the operator given by a SISO static nonlinearity $s : \mathbb{R} \rightarrow \mathbb{R}$, such that for all $u_1, u_2 \in \mathbb{R}$, $y_i \in s(u_i)$,*

$$\mu(u_1 - u_2)^2 \leq (y_1 - y_2)(u_1 - u_2) \leq \lambda(u_1 - u_2)^2. \quad (4)$$

Then the SRG of S is contained within the disc centred at $(\lambda + \mu)/2$ with radius $(\lambda - \mu)/2$.

For a static nonlinearity obeying Condition (4), we say that it is *incrementally in the sector* $[\mu, \lambda]$.

Proof. Define an operator \bar{S} by $u \mapsto \bar{y} := S(u) - \mu u$. Let $\Delta u(t) = u_1(t) - u_2(t)$ and $\Delta \bar{y}(t) = \bar{y}_1(t) - \bar{y}_2(t)$. We drop the t dependence in the remainder of this proof. By assumption on s , for all Δu and corresponding incremental output $\Delta \bar{y}$, we have

$$0 \leq \Delta u(\Delta \bar{y} - \mu \Delta u) \leq (\lambda - \mu) \Delta u^2, \quad (5)$$

$$0 \leq \Delta u \Delta \bar{y} \leq (\lambda - \mu) \Delta u^2. \quad (6)$$

It then follows that $\Delta u \Delta \bar{y} \geq 0$ and $\Delta u \Delta \bar{y} - (\lambda - \mu) \Delta u^2 \leq 0$, from which the following series of equivalent statements follow:

$$\begin{aligned} \Delta u \Delta \bar{y}(\Delta u \Delta \bar{y} - (\lambda - \mu) \Delta u^2) &\leq 0 \\ \Delta u^2(\Delta \bar{y}^2 - (\lambda - \mu) \Delta u \Delta \bar{y}) &\leq 0 \\ \Delta \bar{y}^2 &\leq (\lambda - \mu) \Delta u \Delta \bar{y} \\ \Delta u \Delta \bar{y} &\geq \frac{1}{\lambda - \mu} \Delta \bar{y}^2. \end{aligned}$$

This shows that \bar{S} is output-strict incrementally positive with constant $1/(\lambda - \mu)$, so its SRG is the disc with centre $(\lambda - \mu)/2$ and radius $(\lambda - \mu)/2$. The result then follows by noting that S is the parallel interconnection of \bar{S} with μI , so its SRG is the SRG of \bar{S} shifted to the right by μ . \square

The same bounding region can be obtained for the SG with respect to an input u^* , by restricting the second input in the proof of Proposition 9 to be u^* . This is stated formally below.

Proposition 10. *Suppose $S : L_2 \rightarrow L_2$ is the operator given by a SISO static nonlinearity $s : \mathbb{R} \rightarrow \mathbb{R}$, such that, for all $u_1 \in \mathbb{R}$, $y_1 \in s(u_1)$, $y^* \in s(u^*)$,*

$$\mu(u_1 - u^*)^2 \leq (y_1 - y^*)(u_1 - u^*) \leq \lambda(u_1 - u^*)^2. \quad (7)$$

Then the SG of S with respect to u^ is contained within the disc centred at $(\lambda + \mu)/2$ with radius $(\lambda - \mu)/2$.*

The discs obtained in the previous two propositions are closely related to the discs of the classical incremental circle criterion [40] - indeed, taking the negative and inverting transforms one to the other.

We now show that, for a large class of systems, the disc bound on the SRG cannot be improved. If the characteristic curve of s contains a ‘‘maximal elbow’’, that is, a point where the slope switches from maximum to minimum, then small signals centred around the elbow can be used to generate the perimeter of the bound of Proposition 9. Furthermore, if the region of minimum slope extends to infinity, then large signals can be used to generate the interior of the bound of Proposition 9. This is formalized in the following two propositions. We treat only an elbow from slope 1 to slope 0, as a loop transformation can be used to convert any other elbow to this form.

Proposition 11. *Suppose $S : L_2 \rightarrow L_2$ is a memoryless nonlinearity defined by a map $s : \mathbb{R} \rightarrow \mathbb{R}$ which satisfies (4)*

with $\mu = 0$ and $\lambda = 1$. Furthermore, suppose there are real numbers u^* and $\delta > 0$, such that,

$$s(u^* + \varepsilon_u) - s(u^*) = 0 \text{ for all } \varepsilon_u \in [0, \delta] \quad (8)$$

$$s(u^*) - s(u^* - \varepsilon_l) = \varepsilon_l \text{ for all } \varepsilon_l \in [0, \delta]. \quad (9)$$

Then the SRG of S contains the circle centred at $1/2$ with radius $1/2$.

Proof. We consider two input signals, supported on $[0, 1]$:

$$u_1(t) = u^*, \quad u_2(t) = \begin{cases} u^* + \varepsilon & 0 \leq t < \tau \\ u^* - \varepsilon & \tau \leq t \leq 1, \end{cases}$$

where $\tau \in [0, 1]$. The corresponding output signals are given by

$$y_1(t) = s(u^*), \quad y_2(t) = \begin{cases} s(u^* + \varepsilon) & 0 \leq t < \tau \\ s(u^* - \varepsilon) & \tau \leq t \leq 1, \end{cases}$$

giving the incremental signals

$$\Delta u(t) = \begin{cases} -\varepsilon & 0 \leq t < \tau \\ \varepsilon & \tau \leq t \leq 1, \end{cases} \quad \Delta y(t) = \begin{cases} 0 & 0 \leq t < \tau \\ \varepsilon & \tau \leq t \leq 1. \end{cases}$$

Δy can be written as $k(t)\Delta u(t)$, where

$$k(t) = \begin{cases} 0 & 0 \leq t < \tau \\ 1 & \tau \leq t \leq 1. \end{cases}$$

Calculating gain then gives

$$\|\Delta y\| = \left(\int_0^1 k^2(t) \Delta u^2(t) dt \right)^{\frac{1}{2}} = \left(\int_\tau^1 \Delta u^2(t) dt \right)^{\frac{1}{2}} = \gamma \|\Delta u\|,$$

for some γ which varies between 0 and 1 as τ varies between 1 and 0. It follows that

$$\frac{\|\Delta y\|}{\|\Delta u\|} = \gamma.$$

Calculating the phase gives

$$\begin{aligned} \operatorname{acos} \frac{\langle \Delta u | \Delta y \rangle}{\|\Delta u\| \|\Delta y\|} &= \operatorname{acos} \frac{\int_0^1 k(t) \Delta u^2(t) dt}{\gamma \|\Delta u\|^2} \\ &= \operatorname{acos} \frac{\int_\tau^1 \Delta u^2(t) dt}{\gamma \|\Delta u\|^2} \\ &= \operatorname{acos}(\gamma). \end{aligned}$$

Since $\gamma \in [0, 1]$, we can define ϑ by $\cos(\vartheta) = \gamma$. We then have the locus of points on the SRG given by

$$\cos(\vartheta) \exp(\pm j\vartheta), \quad 0 \leq \vartheta \leq \pi/2,$$

which is the circle with centre $1/2$ and radius $1/2$. \square

Proposition 12. Suppose $S : L_2 \rightarrow L_2$ is a memoryless nonlinearity defined by a map $s : \mathbb{R} \rightarrow \mathbb{R}$ which satisfies (4) with $\mu = 0$ and $\lambda = 1$, and which satisfies $s(0) = 0$. Furthermore, suppose there is a real number u^* such that

$$s(u^* + M) - s(u^*) = 0 \text{ for all } M \geq 0 \quad (10)$$

$$s(u^*) > 0. \quad (11)$$

Then the SRG of S is the disc centred at $s(u^*)/2u^*$ with radius $s(u^*)/2u^*$.

Proof. We consider two input signals, supported on $[0, 1]$:

$$u_1(t) = M, \quad u_2(t) = \begin{cases} M + u^* & 0 \leq t < \tau \\ 0 & \tau \leq t \leq 1, \end{cases}$$

where $\tau \in [0, 1]$, and $M \geq u^*$. Performing the same calculations as in the proof of Proposition 11, and defining $\beta(M) := s(u^*)/M$, we have

$$\begin{aligned} \frac{\|\Delta y\|}{\|\Delta u\|} &= \beta(M)\gamma, \\ \operatorname{acos} \frac{\langle \Delta u | \Delta y \rangle}{\|\Delta u\| \|\Delta y\|} &= \operatorname{acos}(\gamma). \end{aligned}$$

Since $\gamma \in [0, 1]$, we can define ϑ by $\cos(\vartheta) = \gamma$. We then have the locus of points on the SRG given by

$$\beta(M) \cos(\vartheta) \exp(\pm j\vartheta), \quad 0 \leq \vartheta \leq \pi/2.$$

This is the circle with centre $\beta(M)/2$ and radius $\beta(M)/2$. Varying M between u^* and ∞ varies $\beta(M)$ between $s(u^*)/u^*$ and 0, so we fill the disc with centre $s(u^*)/2u^*$ and radius $s(u^*)/2u^*$. \square

Proposition 12 allows us to give an exact characterization of the SRGs of a range of static nonlinearities, including the unit saturation, the ReLU, and the limiting cases of the relay and ideal diode.

The proof of Proposition 11 uses probing signals which have an arbitrarily small magnitude variation about a “worst case” input value. This shows the local or worst case nature of the SRG — the boundary of the SRG is generated by these probing signals.

Remark 1. We conclude this section by remarking that the characterization of output-strict incrementally passive static nonlinearities allows the SRGs of a large class of dynamic output-strict incrementally passive nonlinear systems to be characterized. Output-strict incremental passivity is preserved under negative feedback with an incrementally passive system, as shown in Theorem 3. This means that any scalar system of the form

$$\dot{y} = f(u - y),$$

where f is incrementally in a sector with positive constants, is output-strict incrementally passive. \lrcorner

VII. EXAMPLE 1: FEEDBACK WITH SATURATION AND DELAY

In this section, we use SRGs to analyze feedback systems with delays, dynamic components and static nonlinearities. We will derive incremental stability bounds which depend both on the delay time and the dynamic time constant, similar to the state of the art non-incremental bounds obtained using the roll-off IQC [21]. These bounds are obtained by approximating the SRG of the delay and the dynamics, treated as a single component. In the simple example of this section, where the dynamic component is LTI, this approach reduces to the incremental circle criterion. However, the approach allows for arbitrary dynamic components, as shown in Section IX. One

of the advantages of our approach is the derivation of stability margins and incremental L_2 gain bounds for the closed loop.

We begin with the system of Figure 5, showing a time delay and an LTI transfer function in feedback with a $1/\beta$ -output-strict incrementally passive component Δ .

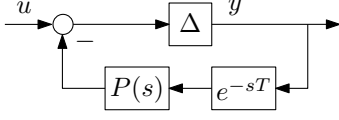


Fig. 5: Simple system with delay in the feedback loop.

We take $P(s) = s^2/(s^3 + 2s^2 + 2s + 1)$, also considered in [13, §3]. The Nyquist diagram of $P(s)$ cascaded with the delay, and a bounding approximation of the SRG, are shown in the left hand side of Figure 6. As the delay is increased, the Nyquist diagram, and hence the SRG, extend further into the left half plane.

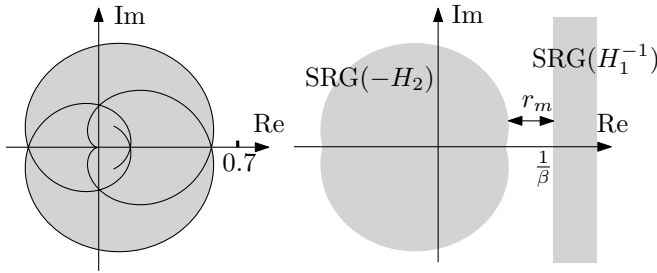


Fig. 6: Left: Nyquist diagram of $e^{-sT}s^2/(s^3 + 2s^2 + 2s + 1)$ (black) and a bounding approximation of its SRG. Right: feedback with $1/\beta$ -output-strict incrementally passive system.

Applying Theorem 2 with $H_2 = e^{-sT}P(s)$ and $H_1 = \Delta$, we obtain the right hand side of Figure 6. Stability is verified if the delay SRG always has real part greater than $1/\beta$, which ensures that $r_m > 0$. Solving numerically for $\min_\omega \text{Re}(P(j\omega)e^{j\omega T})$ gives a stability bound on β , as a function of T , shown in Figure 7, which also shows the non-incremental stability bound obtained by Megretski and Rantzer [13] using IQC analysis, for the particular case where Δ is a saturation. For short delay times, the non-incremental bound is shown to tend to infinity, using the Zames-Falb-O'Shea multiplier. The incremental bound obtained using SRG analysis has a non-smooth point where the leftmost segment of the Nyquist diagram switches, and is bounded for all delay times.

The SRG analysis gives a bound which guarantees finite incremental L_2 gain, a stronger property than the L_2 gain from IQC analysis. Finite incremental L_2 gain in particular implies input-output Lipschitz continuity. To the best of the authors' knowledge (and as also noted in [16]), [15] is the only application of incremental IQCs to stability analysis of feedback systems, with only a very weak form of stability guaranteed. As noted by Kulkarni and Safonov [41], stability results using Zames-Falb-O'Shea and Popov multipliers do not guarantee continuity, as these multipliers do not preserve the incremental passivity of static nonlinear elements. The situation for proving finite incremental L_2 gain with these

multipliers is similar; the loss of incremental passivity of the static nonlinearity means the incremental passivity theorem cannot be applied, so another method of proving stability is needed. One such method would be to apply Theorem 2 to the transformed loop, and indeed there are multipliers which destroy incremental passivity but which still verify an incremental L_2 gain bound. For this particular example, the transfer function $(s+1)/(s-1)$ could be used as a multiplier, although it gives a more conservative bound than Figure 7. Global [16], universal [42] and equilibrium-independent [35] L_2 gain are weaker than incremental L_2 gain but stronger than L_2 gain, and afford differing levels of tractability.

In addition to proving incremental L_2 stability, we can give an incremental L_2 gain bound. For a fixed β , $1/r_m$ is an incremental L_2 gain bound from u to y , which depends on the time delay T . For $\beta = 1$, this bound is plotted in Figure 7.

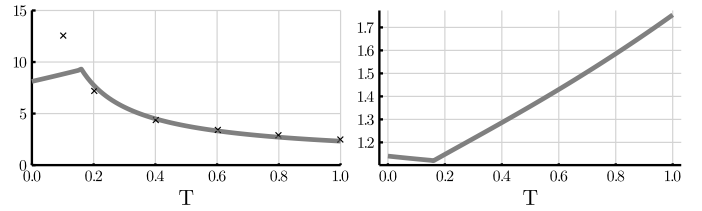


Fig. 7: Left: The grey line is an upper bound on β which guarantees that the system of Figure 5 has bounded incremental L_2 gain with a delay of T . The crosses give a bound on β which guarantees (non-incremental) L_2 stability, obtained using IQC analysis [13, Fig. 6]. Right: the incremental L_2 gain bound from u to y for $\beta = 1$.

The motivation behind the traditional structure of the Lur'e system is to put all of the "troublesome" elements in the nonlinear component, and all of the dynamics in the LTI component. The availability of explicit SRGs for elements which are usually troublesome, such as saturations and delays, means that this structure is not necessarily ideal for SRG analysis, and the feedback system may be better modelled in a different way. This is illustrated in the following two examples.

VIII. EXAMPLE 2: CYCLIC FEEDBACK SYSTEMS

We now turn to the analysis of cascades. Such systems form the basis of cyclic feedback systems, which are often found in biological models [17], among many other application domains (see, for example, the discussion of Mallet-Paret and Sell [18]). In Theorem 5, we give the SRG of a cascade of output-strict incrementally positive systems, which represents a novel system constraint which cannot be represented as an incremental IQC. A gain margin condition applied to a cascade in unity gain negative feedback gives rise to the incremental secant condition [19]. The cascade SRG thus generalizes the incremental secant condition to arbitrary feedback interconnections and disturbances. The result we give here is tight in the sense that stronger conditions than output strict incremental positivity of the plants are required for any stronger bound.

Theorem 5. Consider the cascade of n output-strict incrementally positive systems, with parameters $1/\gamma_i$, $i = 1, \dots, n$,

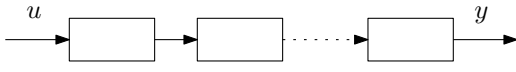


Fig. 8: Cascade of n systems.

shown in Figure 8. The SRG of the cascade is contained within the region with perimeter

$$z(\phi) = \gamma_1 \gamma_2 \dots \gamma_n \left(\cos \frac{\phi}{n} \right)^n e^{-j\phi}, \quad -\pi \leq \phi < \pi. \quad (12)$$

Proof. The SRG of the i^{th} system is the disc with centre $\gamma_i/2$ and radius $\gamma_i/2$. The perimeter of this disc has the parameterization

$$z_i(\vartheta) = \gamma_i \cos(\vartheta) e^{-j\vartheta} \quad -\pi/2 \leq \vartheta < \pi/2 \quad (13)$$

As this disc satisfies the right hand arc property, the SRG of the full cascade is the product of n discs. We claim that the perimeter of this SRG has the parameterization given by Equation 12.

For instance, take any z_1, z_2, \dots, z_n . Using (13) and Proposition 8 gives the point

$$w = \gamma_1 \dots \gamma_n \cos(\vartheta_1) \dots \cos(\vartheta_n) e^{-j(\vartheta_1 + \dots + \vartheta_n)}, \quad (14)$$

for $-\pi < \vartheta_1, \vartheta_2, \dots, \vartheta_n < \pi$. Letting $\vartheta_1 = \vartheta_2 = \dots = \vartheta$, and setting $\phi = n\vartheta$ gives the parameterization (12) (noting that $-\pi \leq \phi < \pi$ as (12) is 2π -periodic). This shows that all the points $z(\phi)$ lie within the SRG. To show that they are indeed on the perimeter of the SRG, we take any point w and show that its magnitude is smaller than the point $z(\phi)$ with the same argument. This follows from (14) if we can show that

$$\cos(\vartheta_1) \cos(\vartheta_2) \dots \cos(\vartheta_n) \leq \cos(\vartheta_1 + \vartheta_2 + \dots + \vartheta_n).$$

This is proved in [19]: $f(\phi) = -\ln \cos(\phi)$ is convex on $(-\pi/2, \pi/2)$. Applying Jensen's inequality gives $f(\sum_i \vartheta_i) \leq \sum_i f(\vartheta_i)$, and the required inequality follows by taking the exponential. Note that the inequality still holds in the limit as one angle $\vartheta_i \rightarrow \pm\pi/2$. \square

The SRG given by Theorem 5 is illustrated in Figure 9. For $n = 2$, this SRG is a special case of [12, Thm. 2]. For $n > 2$, this SRG is a novel result. The intercept with the negative real axis is at the point $z(\pi) = -\gamma_1 \gamma_2 \dots \gamma_n \left(\cos \frac{\pi}{n} \right)^n$. A direct application of Theorem 1 to a cascade in unity gain negative feedback thus gives the following incremental secant condition.

Corollary 3. Suppose the system of Figure 8 is placed in unity gain negative feedback, where the n interconnected systems are each output-strict incrementally positive with parameters γ_i , $i = 1, \dots, n$. The feedback interconnection has a finite incremental L_2 gain if

$$\gamma_1 \gamma_2 \dots \gamma_n < \left(\sec \frac{\pi}{n} \right)^n.$$

To see that the cascade SRG expresses a more general constraint than possible with an incremental IQC, we can take the $n = 2$ case of Equation (12), and eliminate the parameter ϕ .

This gives the following equality constraint on the boundary of the SRG:

$$\langle u_1 - u_2 | y_1 - y_2 \rangle + \|u_1 - u_2\| \|y_1 - y_2\| - 2\|y_1 - y_2\|^2.$$

The middle term cannot be expressed as an incremental IQC.

The cascade SRG allows several other useful values to be computed. An incremental L_2 gain bound can be found by minimizing the distance between -1 and $1/(\gamma_1 \dots \gamma_n \cos(\vartheta_1) \dots \cos(\vartheta_n) e^{-j(\vartheta_1 + \dots + \vartheta_n)})$. This distance is shown for $n = 4$ in Figure 10. Furthermore, we can calculate the shortage of input-strict incremental positivity of the cascade by finding the distance the SRG extends into the left half plane. For example, for a cascade of two systems, the shortage of input-strict incremental positivity is $\gamma_1 \gamma_2 / 8$ [43, p. 118]. Stan *et al.* [44] show that if the coupling strength in a network of oscillators modelled as cascade feedback systems is large enough compared to the shortage of each oscillator, the network will synchronize.

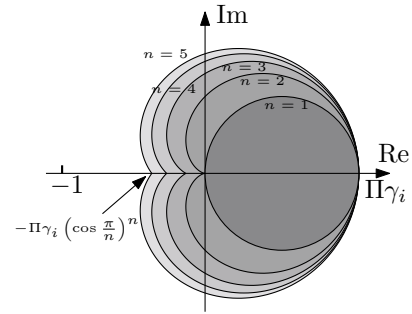


Fig. 9: SRGs of the cascade of Figure 8, where subsystem i is γ_i -output-strict incrementally positive, for 1 to 5 subsystems.

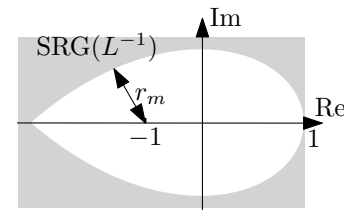


Fig. 10: Inverse SRG of a cascade of four output-strict incrementally positive systems. The stability margin is r_m . The intercept with the negative real axis is at $-1/(\Pi_i \gamma_i (\cos(\pi/n))^n)$.

SRG analysis allows the incremental secant condition to be generalized beyond negative feedback interconnections. For example, if an uncertain gain k_Δ is placed in feedback with the cascade, as shown in Figure 11, we can give a bound on k_Δ for which incremental stability is guaranteed. The inverse SRG of the cascade (Figure 10) is shifted to the left by k_Δ ; if it does not intersect -1 , the closed loop has finite incremental gain. This allows us to conclude stability if

$$(\gamma_1 \gamma_2 \dots \gamma_n)^{-1} > k_\Delta > 1 - \left(\gamma_1 \gamma_2 \dots \gamma_n \left(\cos \frac{\pi}{n} \right)^n \right)^{-1}.$$

Remark 2. Remark 1 showed how the bounding SRG for a static nonlinearity that is incrementally in a sector could be

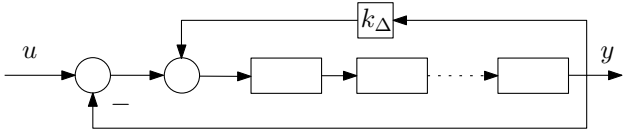


Fig. 11: Cascade of subsystems with an uncertain feedback gain k_Δ , in unity gain negative feedback.

used to determine bounding SRGs for dynamic nonlinearities. The cascade SRG derived in this section allows us to extend this idea to dynamic nonlinearities described by differential equations of the form

$$\dot{y} = f(g(u) - y). \quad (15)$$

Suppose that f is incrementally in the sector $[\mu_1, \gamma_1]$ (in the sense of Proposition 9), and g is incrementally in the sector $[\mu_2, \gamma_2]$. For simplicity, assume $\mu_1 = \mu_2 = 0$. The system of Equation (15) can be represented as f in negative feedback with an integrator, with the nonlinearity g at the input. It follows from Remark 1 and the Theorem 5 that this system has a bounding SRG given by the $n = 2$ case of Figure 9. \square

IX. EXAMPLE 3: COMBINING CASCADES AND DELAYS

In this final example, we combine a delay with a cascade of two output-strict incrementally positive systems, and revisit the Internet congestion control example of Summers, Arcak, and Packard [21]. In that paper, equilibrium-independent IQCs are verified numerically in order to compute a bound on the variables δ , β and N_u in the left of Figure 12, which guarantees (non-incremental) input/output stability of the system. Here, we derive a bound which guarantees finite incremental gain of the system.

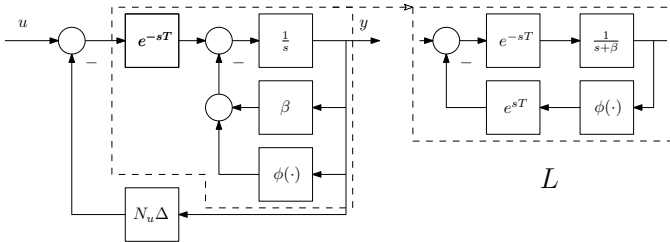


Fig. 12: Left: Internet congestion control example of [21]. $\beta > 0$, $\phi(w)$ is $1/\gamma$ -output-strict incrementally positive, $N_u \in \mathbb{N}$, Δ is δ -output-strict incrementally positive. $0 < \gamma < \beta$. Right: equivalent representation of the forward path, L .

In order to combine the delay and first order lag, we rearrange the forward path as shown in the right of Figure 12. This is the negative feedback interconnection of $H_1 = e^{-sT}/(s + \beta)$ and $H_2 = -e^{sT}\phi(\cdot)$. Bounding SRGs for H_1^{-1} and $-H_2$, illustrated in the top of Figure 13, are derived using Theorem 4, Proposition 1 and Proposition 8. Combining these gives a delay-dependent bounding SRG, shown in the bottom left of Figure 13, for the forward path.

To apply Theorem 2, we solve for the largest radius r as shown in the bottom right of Figure 13, before the two SRGs overlap. This is equal to the reciprocal of the distance

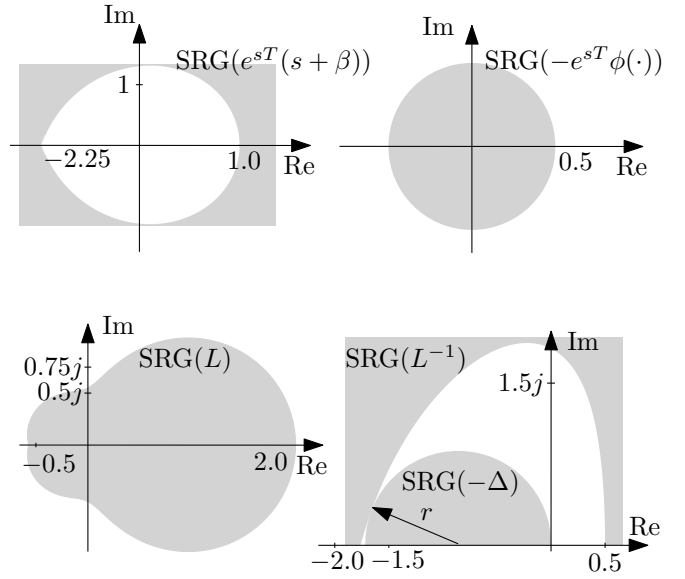


Fig. 13: Top: bounding SRGs for $e^{sT}(s + \beta)$ (left) and $-e^{sT}\phi(\cdot)$ (right), for $\beta = 1$, $T = 1$, $\gamma = 0.5$. Adding these and inverting gives a bounding SRG for L , shown on the bottom left. Bottom right: inverse of L and negative of an r -output-strict incrementally positive block Δ . Only the upper half is shown.

the SRG of L extends into the left half plane, which is solved numerically. This gives the bound on N_u/δ , plotted in Figure 14, that guarantees an incremental L_2 gain bound for the closed loop.

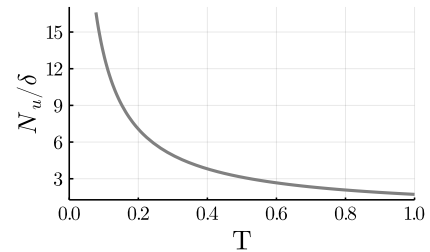


Fig. 14: Upper bound on N_u/δ for the system of Figure 12 to have finite incremental L_2 gain, derived by applying Theorem 2. Plotted for $\beta = 1$, $\gamma = 0.5$.

X. CONCLUSIONS

We have introduced the tool of Scaled Relative Graphs to system analysis, and used it to analyze the incremental stability of operators in feedback. Characterizing stability by the separation of two SRGs unifies existing theorems such as the incremental small gain and passivity theorems, the incremental circle criterion and the incremental secant condition, using an intuitive graphical language. This graphical language is particularly suited to the calculation and visualization of stability margins, and furthermore allows the input-output gain of a feedback system to be estimated. It also allows for a

formulation of H_∞ control design for nonlinear operators. There are many questions for future work; here we will list only a couple.

The SRG composition rules rely on a worst-case assumption: that the *same* signals correspond to the worst-case points in the SRGs of both systems. When dealing with interconnections of individual systems (rather than classes of systems), this can be conservative. For example, applying Theorem 2 to the negative feedback interconnection of $1/(s+1)$ and e^{-sT} does not give a guarantee of stability; we know from the Nyquist criterion, however, that unity-gain negative feedback around $e^{-sT}/(s+1)$ does give a stable system. A second case where the analysis appears to be conservative is in the study of multiple input, multiple output systems. Understanding when SRG analysis is tight, and when it is conservative, is a topic of ongoing research. We expect that twenty years of IQC analysis will contribute to further developing SRG analysis.

A second question is concerned with computation of SRGs. Efficient algorithms for computing or approximating the SRGs of nonlinear operators defined by state space models, or directly from input/output data, are an interesting topic for future research.

A third question is concerned with the extension of the Nyquist theorem to the general case of unstable open loop plants.

The SRG characterization of a system can be tightened by taking the intersection of several bounding SRGs, similar to taking the intersection of several IQCs. SRG analysis also allows a characterization to be *loosened* by taking the union of SRG: for example, a system might *either* be passive, *or* have small gain (or both). This is explored in [45].

We hope that the graphical analysis presented in this paper will further narrow the gap between linear and nonlinear control theory.

APPENDIX I PROOF OF THEOREM 4

The proof has three components. We begin by showing that, for an LTI transfer function $G(s)$, the Nyquist diagram at the frequencies $n2\pi/T$ is a subset of the SRG of $G(s)$. We then show, for operators on the space $L_{2,T}$ of T -periodic, finite energy signals, the SRG is in the convex hull of the points generated by applying the operator to the basis of $L_{2,T}$ given by $\{e^{jtn2\pi/T}\}_{n \in \mathbb{Z}}$, which are exactly the points on the Nyquist diagram. The result then follows by taking the limit as $T \rightarrow \infty$, analogous to the classical derivation of the Fourier transform from the Fourier series.

We begin by observing that the point on the Nyquist diagram of G corresponding to frequency $\omega \in \mathbb{R}$ is precisely $z_G(e^{j\omega t})$. Set $u = ae^{j\omega t}$, then $y = G(u) = \alpha e^{j\omega t + j\psi}$, where $\alpha = |G(j\omega)|$ and $\psi = \angle G(j\omega)$. A direct calculation gives

$$\begin{aligned} \langle u|y \rangle &= \int_0^T u(t)\bar{y}(t)dt \\ &= T\alpha a^2 e^{j\phi}, \\ \|u\| &= \sqrt{T}a, \\ \|y\| &= \sqrt{T}\alpha a, \end{aligned}$$

where $\langle \cdot | \cdot \rangle$ is the inner product on $L_{2,T}$. It follows immediately that

$$z_G(u) = \alpha e^{j\psi},$$

that is, the point on the Nyquist diagram of G corresponding to frequency ω .

The next part of the proof closely follows Huang, Ryu, and Yin [38, Thm 3.1]. In the interests of brevity, we point out only the main arguments and modifications required to that proof.

Let G be an LTI operator on L_2 . The restriction of G to $L_{2,T}$ is then an operator on $L_{2,T}$. Let \mathcal{B} be the set of functions in t given by $\mathcal{B} = \{e^{jtn2\pi/T}, n \in \mathbb{Z}\}$. We show that

$$z_G(\text{span}(\mathcal{B}) \setminus \{0\}) = \text{Poly}(z_G(\mathcal{B})). \quad (16)$$

We begin by noting that \mathcal{B} is an orthonormal basis for $L_{2,T}$, and in particular, for all $u, v \in \mathcal{B}$, $u \neq v$, $\langle v|u \rangle = \langle v|Gu \rangle = \langle Gu|u \rangle = \langle Gu|Gu \rangle = 0$. Therefore, the result of Part 2 of the proof of Huang, Ryu, and Yin [38, Thm. 3.1] holds: for all such u, v , we have

$$z_G(\text{span}(u, v) \setminus \{0\}) = \text{Arc}_{\min}(z_G(u), z_G(v)).$$

The only modification required to the proof is that the inner product here is complex valued, and the real part must be taken. Parts 3 and 4 of the proof of Huang, Ryu, and Yin [38, Thm. 3.1] show that $z_G(\text{span}(\mathcal{B}) \setminus \{0\}) \subseteq \text{Poly}(z_G(\mathcal{B}))$ and $z_G(\text{span}(\mathcal{B}) \setminus \{0\}) \supseteq \text{Poly}(z_G(\mathcal{B}))$ respectively, with the proof requiring only the additional fact that $\text{Poly}(S)$ (in the proof of [38, Thm. 3.1]) is defined for a countably infinite set, as described in Section V-A. This concludes the second part of the proof: $z_G(\text{span}(\mathcal{B}) \setminus \{0\}) = \text{Poly}(z_G(\mathcal{B}))$.

Finally, we extend to aperiodic signals by letting the period $T \rightarrow \infty$ and the fundamental frequency $2\pi/T \rightarrow 0$. In the interests of brevity, we give the proof here assuming that the Fourier transform of the input $u(t)$ is Riemann integrable. The result can be extended to arbitrary functions on L_2 using the same machinery for defining the Fourier transform on L_2 - see, for instance, Rudin [46, Chap. 9]. We first note that $z_G(ae^{i\omega t})$ may be computed using the inner product and norm on L_2 , rather than $L_{2,T}$, as a limit, and the result will be unchanged. Let $u(t)$ be an input signal on L_2 , and $y(t)$ the corresponding output. The Fourier inversion theorem gives

$$y(t) = \frac{1}{\sqrt{2\pi}} \int_{-\infty}^{\infty} G(j\omega) \hat{u}(\omega) e^{j\omega t} d\omega. \quad (17)$$

Let

$$\frac{\Delta\omega}{\sqrt{2\pi}} \sum_{n=-\infty}^{\infty} G(jn\Delta\omega) \hat{u}(n\Delta\omega) e^{jn\Delta\omega t}$$

be a Riemann sum approximation of the right hand side of (17), with uniform spacing $\Delta\omega$. By (16), we know this sum belongs to $\text{Poly}(\{G(j\Delta\omega)e^{jn\Delta\omega t}\}_{n \in \mathbb{Z}}) \subseteq \text{Poly}(\{G(j\omega)e^{j\omega t}\}_{\omega \in \mathbb{R}})$. Letting $\Delta\omega \rightarrow 0$, we have that the right hand side of (17) belongs to $\text{Poly}(\{G(j\omega)e^{j\omega t}\}_{\omega \in \mathbb{R}})$, noting that the restriction of the Nyquist diagram to $\mathbb{C}_{\text{Im} \geq 0}$ is compact in \mathbb{C} . Note that this is precisely the h-convex hull of the Nyquist diagram of G . \square

REFERENCES

- [1] A. El-Sakkary, "The gap metric: Robustness of stabilization of feedback systems," *IEEE Transactions on Automatic Control*, vol. 30, no. 3, pp. 240–247, 1985. DOI: 10.1109/TAC.1985.1103926.
- [2] G. Vinnicombe, *Uncertainty and Feedback: H_∞ Loop-Shaping and the ν -Gap Metric*. Imperial College Press, 2000, ISBN: 978-1-86094-163-4.
- [3] G. Zames, "Feedback and optimal sensitivity: Model reference transformations, multiplicative seminorms, and approximate inverses," *IEEE Transactions on Automatic Control*, vol. 26, no. 2, pp. 301–320, 1981. DOI: 10.1109/TAC.1981.1102603.
- [4] C. A. Desoer and M. Vidyasagar, *Feedback Systems: Input-Output Properties*. Elsevier, 1975. DOI: 10.1016/b978-0-12-212050-3.x5001-4.
- [5] N. S. Krylov and N. N. Bogoliubov, *Introduction to Non-Linear Mechanics*. Princeton: Princeton University Press, 1947, ISBN: 978-0-691-07985-1.
- [6] A. Blagquière, *Nonlinear System Analysis*. Academic Press, 1966.
- [7] J.-J. E. Slotine and W. Li, *Applied Nonlinear Control*. Englewood Cliffs, N.J: Prentice Hall, 1991, 459 pp., ISBN: 978-0-13-040890-7.
- [8] A. Pavlov, N. van de Wouw, and H. Nijmeijer, "Frequency response functions and Bode plots for nonlinear convergent systems," in *Proceedings of the 45th IEEE Conference on Decision and Control*, San Diego, CA, USA: IEEE, 2006, pp. 3765–3770. DOI: 10.1109/CDC.2006.377669.
- [9] C. Chen, D. Zhao, W. Chen, S. Z. Khong, and L. Qiu, "Phase of nonlinear systems," 2020. arXiv: 2012.00692 [cs, eess, math].
- [10] C. Chen, W. Chen, D. Zhao, S. Z. Khong, and L. Qiu, "The singular angle of nonlinear systems," Sep. 3, 2021. arXiv: 2109.01629 [cs, eess, math].
- [11] E. K. Ryu, R. Hannah, and W. Yin, "Scaled relative graphs: Non-expansive operators via 2D Euclidean geometry," *Mathematical Programming*, 2021. DOI: 10.1007/s10107-021-01639-w.
- [12] X. Huang, E. K. Ryu, and W. Yin, "Tight coefficients of averaged operators via scaled relative graph," *Journal of Mathematical Analysis and Applications*, vol. 490, no. 1, 2020. DOI: 10.1016/j.jmaa.2020.124211.
- [13] A. Megretski and A. Rantzer, "System analysis via integral quadratic constraints," *IEEE Transactions on Automatic Control*, vol. 42, no. 6, pp. 819–830, 1997. DOI: 10.1109/9.587335.
- [14] T. Chaffey, F. Forni, and R. Sepulchre, "Scaled relative graphs for system analysis," in *2021 60th IEEE Conference on Decision and Control (CDC)*, Austin, TX, USA: IEEE, 2021, pp. 3166–3172. DOI: 10.1109/CDC45484.2021.9683092.
- [15] U. T. Jonsson, Chung-Yao Kao, and A. Megretski, "A semi-infinite optimization problem in harmonic analysis of uncertain systems," in *Proceedings of the 2001 American Control Conference*, vol. 4, 2001, 3029–3034 vol.4. DOI: 10.1109/ACC.2001.946379.
- [16] R. Wang and I. R. Manchester, "Robust contraction analysis of nonlinear systems via differential IQC," in *2019 IEEE 58th Conference on Decision and Control (CDC)*, Nice, France: IEEE, Dec. 2019, pp. 6766–6771, ISBN: 978-1-72811-398-2. DOI: 10.1109/CDC40024.2019.9029867.
- [17] J. J. Tyson and H. G. Othmer, "The dynamics of feedback control circuits in biochemical pathways," in *Progress in Theoretical Biology*, Elsevier, 1978, pp. 1–62, ISBN: 978-0-12-543105-7.
- [18] J. Mallet-Paret and G. R. Sell, "The Poincaré–Bendixson Theorem for monotone cyclic feedback systems with delay," *Journal of Differential Equations*, vol. 125, no. 2, pp. 441–489, 1996, ISSN: 0022-0396. DOI: 10.1006/jdeq.1996.0037.
- [19] E. D. Sontag, "Passivity gains and the "secant condition" for stability," *Systems & Control Letters*, vol. 55, no. 3, pp. 177–183, 2006. DOI: 10.1016/j.sysconle.2005.06.010.
- [20] M. Arcak and E. D. Sontag, "Diagonal stability of a class of cyclic systems and its connection with the secant criterion," *Automatica*, vol. 42, no. 9, pp. 1531–1537, 2006, ISSN: 0005-1098. DOI: 10.1016/j.automatica.2006.04.009.
- [21] E. Summers, M. Arcak, and A. Packard, "Delay robustness of interconnected passive systems: An integral quadratic constraint approach," *IEEE Transactions on Automatic Control*, vol. 58, no. 3, pp. 712–724, 2013. DOI: 10.1109/TAC.2012.2219972.
- [22] G. Zames, "On the input-output stability of time-varying nonlinear feedback systems, part one: Conditions derived using concepts of loop gain, conicity, and positivity," *IEEE Transactions on Automatic Control*, vol. 11, no. 2, pp. 228–238, 1966. DOI: 10.1109/tac.1966.1098316.
- [23] J. C. Willems, *The Analysis of Feedback Systems*, ser. The MIT Press Research Monograph Series, No. 62. Cambridge, Mass: The MIT Press, 1971, ISBN: 978-0-262-23046-9.
- [24] J. W. Polderman and J. C. Willems, *Introduction to Mathematical Systems Theory: A Behavioral Approach*. Springer Science & Business Media, 1997, vol. 26, ISBN: 0-387-98266-3.
- [25] G. Zames, "Nonlinear operators of system analysis," Massachusetts Institute of Technology, 1960.
- [26] I. Sandberg, "Some results on the theory of physical systems governed by nonlinear functional equations," *The Bell System Technical Journal*, 1965.
- [27] R. J. Duffin, "Nonlinear networks. I," *Bulletin of the American Mathematical Society*, vol. 52, no. 10, pp. 833–839, 1946.
- [28] G. J. Minty, "Monotone networks," *Proceedings of the Royal Society of London. Series A. Mathematical and Physical Sciences*, vol. 257, no. 1289, pp. 194–212, 1960. DOI: 10.1098/rspa.1960.0144.
- [29] —, "On the maximal domain of a "monotone" function," *The Michigan Mathematical Journal*, vol. 8, no. 2, pp. 135–137, 1961. DOI: 10.1307/mmj/1028998564.
- [30] R. T. Rockafellar, "Monotone operators and the proximal point algorithm," *SIAM Journal on Control and Optimization*, vol. 14, no. 5, pp. 877–898, 1976. DOI: 10.1137/0314056.
- [31] E. K. Ryu and S. Boyd, "A primer on monotone operator methods," *Appl. Comput. Math.*, vol. 15, no. 1, pp. 3–43, 2016.
- [32] E. K. Ryu and W. Yin, *Large-Scale Convex Optimization via Monotone Operators*, Draft. 2022.
- [33] P. L. Combettes and J.-C. Pesquet, "Proximal splitting methods in signal processing," in *Fixed-Point Algorithms for Inverse Problems in Science and Engineering*, ser. Springer Optimization and Its Applications, H. H. Bauschke, R. S. Burachik, P. L. Combettes, V. Elser, D. R. Luke, and H. Wolkowicz, Eds., New York, NY: Springer, 2011, pp. 185–212. DOI: 10.1007/978-1-4419-9569-8_10.
- [34] P. L. Combettes, "Monotone operator theory in convex optimization," *Mathematical Programming*, vol. 170, no. 1, pp. 177–206, 2018. DOI: 10.1007/s10107-018-1303-3.
- [35] G. H. Hines, M. Arcak, and A. K. Packard, "Equilibrium-independent passivity: A new definition and numerical certification," *Automatica*, vol. 47, no. 9, pp. 1949–1956, 2011. DOI: 10.1016/j.automatica.2011.05.011.
- [36] J. C. Doyle, B. A. Francis, and A. R. Tannenbaum, *Feedback Control Theory*. Courier Corporation, 1992.
- [37] R. Pates, "The scaled relative graph of a linear operator," 2021. arXiv: 2106.05650 [math].
- [38] X. Huang, E. K. Ryu, and W. Yin, "Scaled relative graph of normal matrices," 2020. arXiv: 2001.02061 [cs, math].
- [39] R. T. Rockafellar and R. J. B. Wets, *Variational Analysis*, ed. by M. Berger, P. de la Harpe, F. Hirzebruch, N. J. Hitchin, L. Hörmander, A. Kupiainen, G. Lebeau, M. Ratner, D. Serre, Y. G. Sinai, N. J. A. Sloane, A. M. Vershik, and M. Waldschmidt, ser. Grundlehren Der Mathematischen Wissenschaften. Berlin, Heidelberg: Springer Berlin Heidelberg, 1998, vol. 317, ISBN: 978-3-540-62772-2. DOI: 10.1007/978-3-642-02431-3.
- [40] G. Zames and P. L. Falb, "Stability conditions for systems with monotone and slope-restricted nonlinearities," *SIAM Journal on Control*, vol. 6, no. 1, pp. 89–108, 1968. DOI: 10.1137/0306007.
- [41] V. V. Kulkarni and M. G. Safonov, "Incremental positivity non-preservation by stability multipliers," in *Proceedings of the 40th IEEE Conference on Decision and Control*, vol. 1, 2001, 33–38 vol.1. DOI: 10.1109/CDC.2001.980064.
- [42] I. R. Manchester and J.-J. E. Slotine, "Robust control contraction metrics: A convex approach to nonlinear state-feedback H_∞ control," *IEEE Control Systems Letters*, vol. 2, no. 3, pp. 333–338, 2018, ISSN: 2475-1456. DOI: 10.1109/LCSYS.2018.2836355.
- [43] J. D. Lawrence, *A Catalog of Special Plane Curves*. Courier Corporation, Jan. 1, 1972, ISBN: 978-0-486-60288-2.
- [44] G.-B. Stan, A. Hamadeh, R. Sepulchre, and J. Goncalves, "Output synchronization in networks of cyclic biochemical oscillators," in *IEEE American Control Conference*, 2007, pp. 3973–3978. DOI: 10.1109/ACC.2007.4282673.
- [45] T. Chaffey, "A rolled-off passivity theorem," *Systems & Control Letters*, vol. 162, p. 105 198, Apr. 1, 2022, ISSN: 0167-6911. DOI: 10.1016/j.sysconle.2022.105198.
- [46] W. Rudin, *Real and Complex Analysis*, 3rd ed. New York: McGraw-Hill, 1987, 416 pp., ISBN: 978-0-07-054234-1.



Thomas Chaffey (S17) received the B.Sc. (adv-math) degree in mathematics and computer science in 2015 and the M.P.E. degree in mechanical engineering in 2018, from the University of Sydney, Australia, and the Ph.D. degree in engineering from the University of Cambridge, UK, in 2022. He currently holds the Maudslay–Butler Research Fellowship at Pembroke College, University of Cambridge. His research interests are in nonlinear systems, circuits and optimization.

He received the Best Student Paper Award at the 2021 European Control Conference and the Outstanding Student Paper Award at the 2021 IEEE Conference on Decision and Control.



Fulvio Forni received the Ph.D. degree in computer science and control engineering from the University of Rome Tor Vergata, Rome, Italy, in 2010. In 2008–2009, he held visiting positions with the LFCS, University of Edinburgh, U.K. and with the CCDC of the University of California Santa Barbara, USA. In 2011–2015, he held a post-doctoral position with the University of Liege, Belgium (FNRS). He is currently a Lecturer with the Department of Engineering, University of Cambridge, U.K. Dr. Forni was a

recipient of the 2020 IEEE CSS George S. Axelby Outstanding Paper Award.



Rodolphe Sepulchre (M96,SM08,F10) received the engineering degree and the Ph.D. degree from the Université catholique de Louvain in 1990 and in 1994, respectively. He is Professor of engineering at Cambridge University since 2013. His research interests are in nonlinear control and optimization, and more recently neuromorphic control. He co-authored the monographs "Constructive Nonlinear Control" (Springer-Verlag, 1997) and "Optimization on Matrix Manifolds" (Princeton

University Press, 2008). He is Editor-in-Chief of IEEE Control Systems. In 2008, he was awarded the IEEE Control Systems Society Antonio Ruberti Young Researcher Prize. He is a fellow of IEEE, IFAC, and SIAM. He has been IEEE CSS distinguished lecturer between 2010 and 2015. In 2013, he was elected at the Royal Academy of Belgium.